



The effect of solution pH on the oscillatory electro-oxidation of methanol

Gabriel B. Melle^a, Fabian W. Hartl^b, Hamilton Varela^b, Elton Sitta^{a,*}

^a Federal University of Sao Carlos, Rod. Washington Luis km 235, CEP 13565-905 Sao Carlos, SP, Brazil

^b Institute of Chemistry of Sao Carlos, Av. Trabalhador São-carlense 400, CEP 13566-956 Sao Carlos, SP, Brazil



ARTICLE INFO

Keywords:

Methanol
Electro-oxidation
pH
Oscillations
Dynamic instabilities

ABSTRACT

The methanol electro-oxidation reaction (MER) was studied in a wide pH range under voltammetric and oscillatory regimes. Employing buffered hydrogen phosphates solutions, it was demonstrated that increasing the pH MER is firstly inhibited in the region up to 4–5 but after this point starts to increase reaching currents 5 times bigger than those in acidic media. Potential oscillations during MER are restricted to the pH < 3.5. While the oscillations frequency and shape change slightly in the studied pH range, the amplitude and poisoning rate, calculated in terms of dE/dt , are severely affected by the pH, culminating in the extinguishment of oscillations.

1. Introduction

Oscillations in electrochemical systems have been extensively studied in the last decades and the electro-oxidation of small organic molecules has received special attention due to possible application in energy conversion devices, such as direct alcohol fuel cells [1–3]. These oscillations are caused by coupled feedback loops responsible for the autocatalytic increase of potential (positive loop) followed by slower processes (negative loops) that restore the initial conditions. At a molecular level, the incomplete electro-oxidation of small organic molecules leads to surface poisoning over time, requiring an overpotential to maintain the reaction rate constant in experiments under current control. In some potential regions (known as N-NDR – *N-shaped* Negative Differential Resistance), the overpotential induces the increase of surface poisoning leading to a new increase of overpotential until the surface becomes capable to adsorb oxygenated species that react with the poisons. Once oxidized the poisons leave the surface and the potential decreases, restoring the system to the (nearly) initial conditions [3]. Since the N-NDR region is usually partially hidden, the oscillatory electro-oxidation of small organic molecules are classified as HN-NDR (hidden *N-shaped* negative differential resistance) [4].

Both positive and negative feedback loops are influenced by the experimental conditions, such as applied current, temperature, electro-sorbing species, reaction spectators and solution pH (see [1,2,5] and references therein). Concerning the latter parameter, it is generally accepted that the electro-oxidation of organic molecules is more facile in alkaline media [6–8]. Still not fully understood, this behavior has been addressed to the replacement of adsorbable electrolyte anions by OH^- [9], the reactivity of $\text{CH}_{x,\text{ad}}$ [7] or mechanisms involving small

concentrations but highly reactive alkoxides [10]. Oscillations are strongly affected by the solution pH as clearly discernible in the oscillatory amplitude, frequencies or waveform during the electro-oxidation of formic acid/formate [11,12], ethanol [13,14], ethylene glycol [6,15] and glycerol [16] in acidic and alkaline media. In particular, oscillations were mapped for the electro-oxidation of formic acid/formate [12] and ethylene glycol (EG) [6] in a wide pH range. In both cases oscillations are present in pH < 4 and > 12. Acidic media allows slow frequency high amplitude oscillations in the EG electro-oxidation reaction [6], whereas in alkaline media, the frequencies and amplitude are increased (3–5 times) and decreased (2–3 times), respectively.

Interestingly, besides the oscillatory methanol electro-oxidation reaction (MER) representing one of the most studied systems in acidic media [17–23], we found just one example of oscillatory kinetics in alkaline media, however catalyzed by Ni oxides at potentials around the region of oxygen evolution reaction [24]. It is well established in the literature, that MER occurs via a dual pathway mechanism consisting of poisoning and active species [25,26]. Adsorbed carbon monoxide has been identified as the main poison at low potentials, requiring the adsorption of oxygenated species to be oxidized to CO_2 . Formaldehyde and formic acid are side reaction products that, due to their reactivity, they can also re-adsorb contributing to the $\text{CO}_{\text{ad}} \rightarrow \text{CO}_2$ pathway. The electrolyte pH influences both the amounts and the reactivity of these species (see the discussion below), in this sense, a 1967 study performed by Bagotzky and Vassilyev [8] had already pointed out the importance of pH on methanol oxidation rates observing an activity increase with the pH. Moreover, Abruña et al. [27] and Varela et al. [19,28] estimated the apparent activation energy ($E_{a,\text{app}}$) based on CV currents at potentials below 0.9 V. They obtained values of about

* Corresponding author.

E-mail address: esitta@ufscar.br (E. Sitta).

<https://doi.org/10.1016/j.jelechem.2018.08.033>

Received 2 May 2018; Received in revised form 2 August 2018; Accepted 22 August 2018

Available online 24 August 2018

1572-6657/ © 2018 Elsevier B.V. All rights reserved.

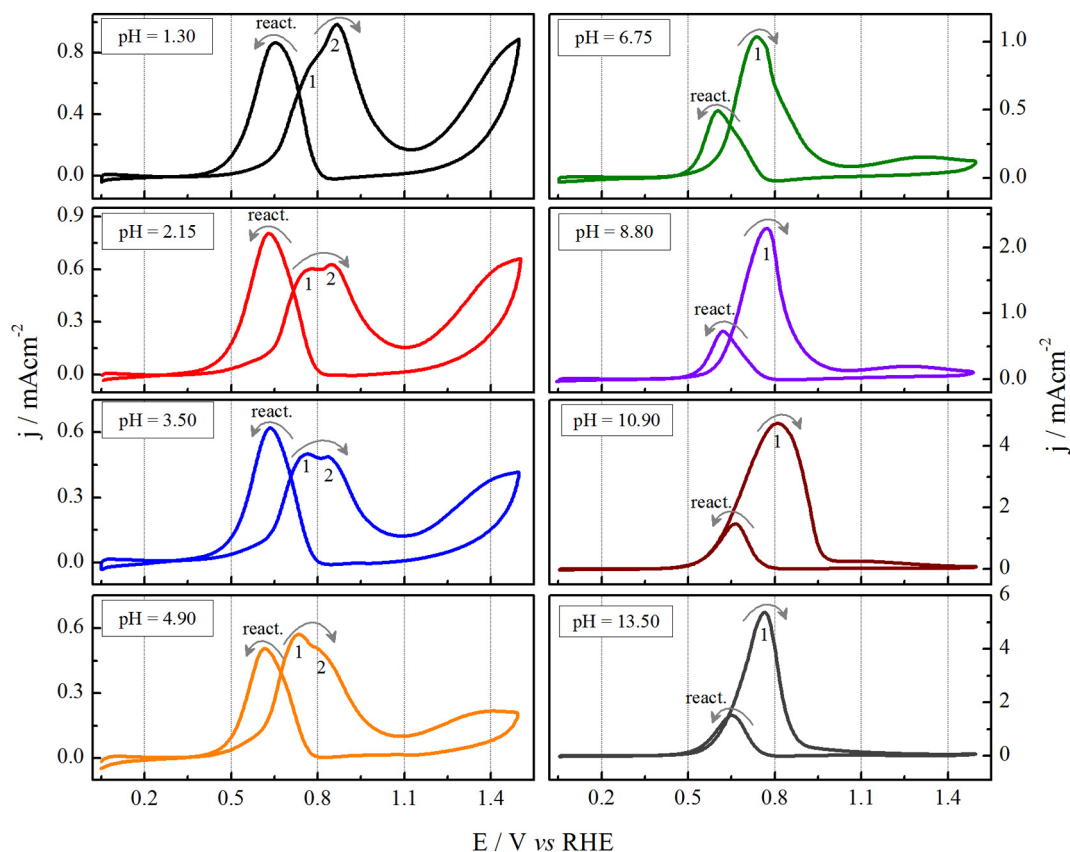


Fig. 1. Pt cyclic voltammograms at distinct pH values, 0.05 V s^{-1} and 0.5 mol L^{-1} methanol. The grey arrows indicate the sweep direction and the notation 1, 2 and react. Indicate the peaks 1, 2 and reactivation, respectively. $T = 25^\circ \text{C}$.

67–90 kJ mol^{-1} in acidic (H_2SO_4 0.5 mol L^{-1}) and 15–40 kJ mol^{-1} in alkaline (KOH 0.1 mol L^{-1}) media, suggesting distinct reaction pathways. In situ Fourier-transform infrared spectroscopy (FTIRs) experiments have shown the presence of both linear and bridged bond CO_{ad} at low potentials, regardless the pH, i.e. strong acidic [29,30] or alkaline [31,32] media. Bands assigned to formate ions are also observed indicating the changes in pH does not cease pathways, but probably acts on the amount and reactivity of intermediates. For instance, steady-state CO coverage values from methanol adsorption is ca 0.40 ML in 0.1 mol L^{-1} H_2SO_4 and 0.28 ML in 0.1 mol L^{-1} NaOH [9], a small difference considering the pH range, but these values could be sufficient to trigger changes in the oscillatory behavior.

The reactivity of MER intermediates depict several changes over a wide pH range; for example, in the pH region between 2 and 4, the first CO electro-oxidation stages are not affected by the pH, but for $\text{pH} > 4$, all peak positions were negatively shifted, indicating a catalytic effect provided by alkaline media when compared with acid [33]. Hydrogen phosphates, CO and OH adsorption strength or even the dependence of CO_{ad} surface mobility on the solution pH could also play a role in the overall process [34–38]. The electro-oxidation of formic acid also strongly depends on the pH, but the behavior differs from the other organic molecules, i.e. the activity increases with the pH until the formate/formic acid pK_a value (3.75), then the activity remains high until pH 10 if a weak adsorbing anions electrolyte is employed or quickly decreases in solutions containing hydrogen phosphate or Cl^- [39,40]. In situ FTIRs in the ATR configuration indicated the presence of both linear and bridge-bonded CO throughout all the studied pH range under voltammetric conditions, but bridge-bonded adsorbed formate is present only in $\text{pH} < \sim 5$ [41].

While CO_{ad} formation and anion adsorption are probably acting as main poisoning species during oscillatory electro-oxidation of small organic molecules in acidic media, increasing the alkalinity, the

mechanism of surface poisoning becomes unclear and could be even caused by the high surface interaction with OH/O species. Anyway, while the oxidation peak currents increase for ethylene glycol [6,15] and glycerol [16,42] with the pH (> 10 times from H_2SO_4 1.0 mol L^{-1} to KOH 1.0 mol L^{-1}), for formic acid the opposite behavior is depicted at $\text{pH} > 4$ [40]. Thus, even recognizing some common intermediates it is very difficult to draw up a general mechanism to explain or preview the oscillatory behavior in a wide pH range.

In the present work we report an experimental study of the MER catalyzed by Pt in a wide pH range provided by buffered phosphate solutions. Oscillatory kinetic regions were mapped and compared with other small organic molecules.

2. Experimental

The experiments were conducted in a three electrodes cell, with working and counter electrodes consisting of Pt band (0.8 cm^2 measured by the oxidation charge of H_{UPD} region) and high area Pt mesh, respectively. At pH under 2 or over 12, a same solution reversible hydrogen electrode (RHE) served as potential reference. For intermediates pHs an $\text{Ag}/\text{AgCl}/\text{KCl}_{\text{sat}}$ electrode connected to the supporting electrolyte through a Luggin capillary was employed, but the results are shown on the RHE scale. Supporting electrolytes were prepared with a buffered solution composed of $\text{H}_3\text{PO}_4/\text{NaH}_2\text{PO}_4/\text{Na}_2\text{HPO}_4/\text{Na}_3\text{PO}_4/\text{NaOH}$ (Sigma-Aldrich, ACS reagent) in distinct proportions to obtain the desired pH always keeping Na^+ concentration at 0.5 mol L^{-1} . An exception was the solution of pH 1.30 composed of 0.5 mol L^{-1} H_3PO_4 in absence of Na^+ .

Before the experiments a cyclic voltammogram from 0.05 to 1.50 V (vs RHE) in a N_2 purged supporting electrolyte attested to the cleanness of the systems. Thereafter methanol was inserted directly into the cell yielding 0.5 mol L^{-1} . Cyclic voltammograms at 0.1 V s^{-1} until current-

potential profile stabilization were performed, which were set as pre-treatment before every measurement run. An Autolab PGSTAT128N equipped with scan250 served as potentiostat/galvanostat and the temperature was maintained at 25 °C using a thermostatic bath (Solab SL 152).

3. Results and discussion

Fig. 1 shows cyclic voltammograms (CV) for MER at distinct pH values as indicated in the panels. For a pH below 6, two oxidation peaks are discernible along the positive going scan around 0.73 and 0.80 V, named peak 1 and 2, respectively. At $E > 1.1$ V methanol oxidation prevails over a platinum oxide layer. At pH 1.30 peak 1 is observed as a shoulder and increases with pH, becoming more intense than peak 2 at pH 3.50. Considering this behavior, it was admitted that the single peaks observed at $pH > 6$ correspond to the process at 0.73 V in acid media and peak 2 is not discernible in alkaline media. The onset of MER is monotonically shifted by the pH, reaching ca 0.1 V from pH 1.30 to 13.50, meanwhile no clear tendency was observed on the potential of the peaks (see Fig. S1).

The negative going scans are described by single oxidation current peak, usually called reactivation peak, regardless of the pH, nevertheless, the position of these processes in comparison with peaks in positive going scan (hysteresis) is pH dependent, for example, in the potential region of pre-peak 1 (from 0.5 to 0.75 V). In strong acidic media the oxidation currents during the positive going scan are lower than those in the negative one. However, the behavior is inverted, as the pH increase. Thus, at low pH the adsorbed species at low potential seems to shift the peak's onset to high overpotentials. The higher currents in the negative going scan are accomplished due to the oxide layer in the potential region before the reactivation peak, avoiding thus strong adsorbed intermediates of MER or anions from electrolyte.

Focusing on the processes taking place at $E < 1.0$ V, Fig. 2(a) presents the maximum current values (j_{pot}) of peaks 1, 2 and the reactivation peak in function of the pH. The values were directly extracted from the CV and no deconvolution was employed. The general behavior can be divided into two regions: (1) the current values of the peak slightly decrease from 1.30 to 3.50 with the reactivation values higher than peak 1; (2) at $pH > 5$, peak 2 disappears and peak 1 starts to increase, giving a 0.15 reaction order in respect to OH^- ($n_{OH^-} = \frac{\partial \log i}{\partial pH}$) in the pH region between 4.9 and 11. In the second region, the reactivation peak also becomes lower than peak 1.

Performing the MER under current control, Fig. 3 presents current sweeps (galvanodynamic curves) at $3.8 \mu A s^{-1} cm^{-2}$ showing how the potential evolves to yield the desired currents. Potentials higher than 0.50 V are necessary to maintain currents higher than $50 \mu A cm^{-2}$, regardless of the electrolyte pH. However, once reaching the region corresponding to the onset of peak 1, the potential increases slowly until ca. 0.80 V, where it suddenly jumps to $E > 1.20$ V. The current needed for this jump can be also compared with the peak current in CV of Fig. 1 and their values are shown in Fig. 2(b) as j_{galv} . Remarkably, the two above-mentioned regions are also present under current control. Finally, the most interesting features are observed at pH 1.3, 2.15 and 3.50, i.e. the potential oscillations preceding the potential jump. The inset in Fig. 3 highlights these features and their analysis.

The minimum in the current values around pH 4, c.f. Fig. 2, coincides with the changes in both CO and formic acid electro-oxidation mechanism described on Introduction section. CO_{ad} electro-oxidation seems to be pH independent for $pH < 4$ and it is catalyzed above this value [33], which could be an explanation to the increase of MER. The behavior for the MER in the studied pH range is opposite to that for formic acid, i.e. the activity for MER is lowest in the pH region of maximum activity for formic acid electro-oxidation in similar electrolyte conditions [40,43]. The formic acid adsorption (as bridged formate) is pH dependent and could be also influenced by or influencing

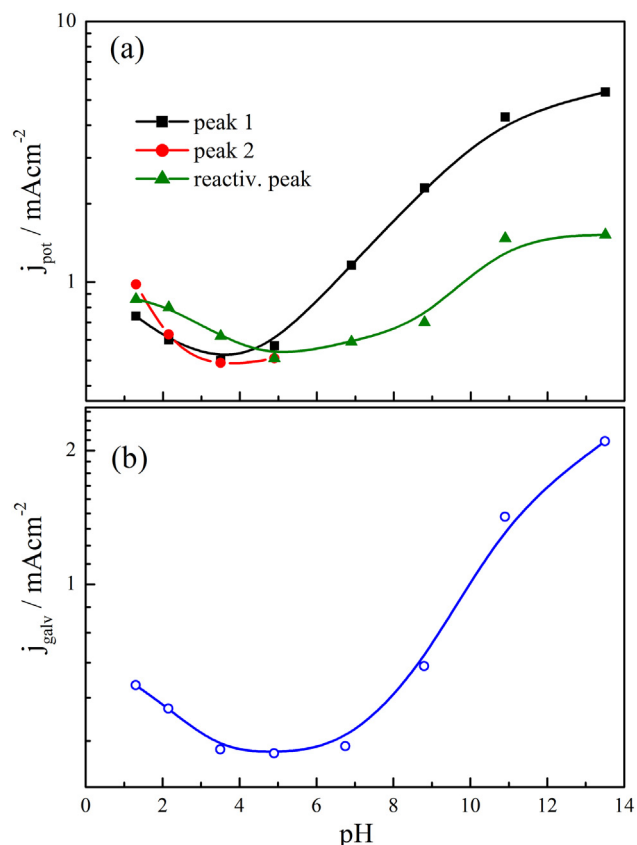


Fig. 2. (a) Peak intensities extracted from the cyclic voltammograms of Fig. 1. Peak 1 and 2 represent the peaks at potential ca. 0.73 and 0.80 V, respectively and the reactiv. peak represents the maximum currents in reactivation region on the negative going sweep. (b) Maximum current reached in galvanodynamic sweep before potential jump to $E > 1.20$ V (details in Fig. 3). The currents are displayed in the log scale.

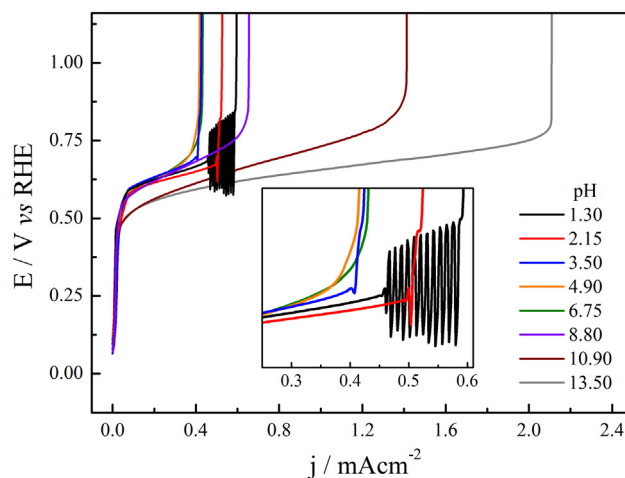


Fig. 3. Galvanodynamic curves at $3.8 \mu A s^{-1} cm^{-2}$ for distinct pH values during MER under the identical conditions as in Fig. 1. The inset highlights the potential instabilities.

MER. Moreover, this pH region corresponds to the higher relative amount of $H_2PO_4^-$ in the electrolyte [44], which could be exerting some effect on the indirect $methanol \rightarrow CO_{ad} \rightarrow CO_2$ and/or in the direct pathway [30,45]. To the best of our knowledge there are no studies on the effect of these ions on oxide formation or methanol adsorption dynamics on surfaces.

Oscillations during the MER were found to be restricted to the pH

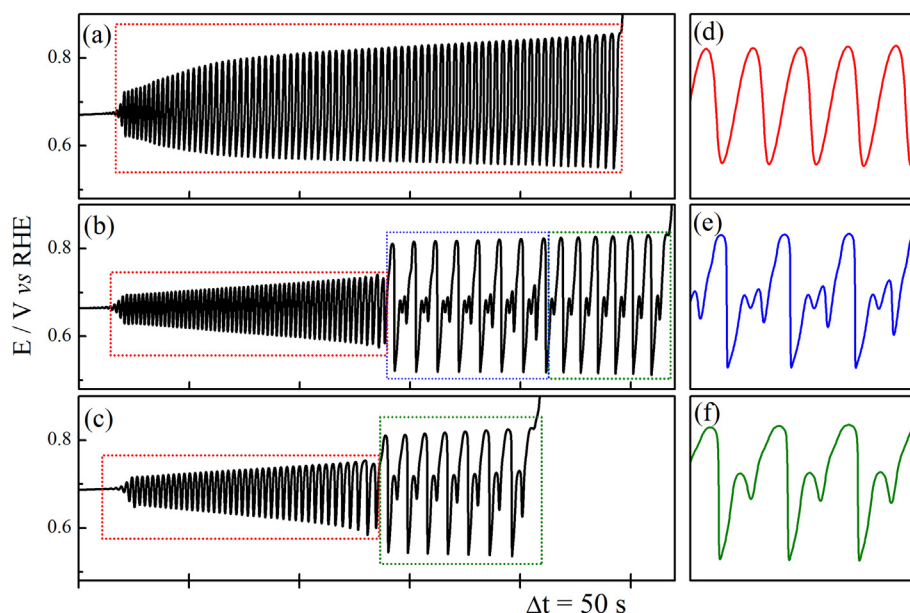


Fig. 4. Galvanostatic time series for methanol electrooxidation in pH 1.30 (a), 2.15 (b) and 3.50 (c) at 0.53 , 0.50 and 0.40 mA cm^{-2} ($j_N = 0.5$), respectively. The dotted boxes correlate the presence of patterns shown in (d)–(f) panels in the series.

region in Fig. 2 in which both peak 1 and 2 are discernible and its intensity (current) decreases with the pH. As mentioned in the introduction, the oscillatory mechanism involves the competition between poisoned and active species in the same potential window and small changes in the surface population can extinguish the oscillations. The region in which the oscillations are present in Fig. 3 strongly decreases with pH, giving just a small instability at pH 3.5. Employing the normalization procedure described in ref. [46], we set currents in the oscillatory region and the potential behavior evolves in time as given in Fig. 4. Currents were also set near the potential jump on $\text{pH} > 3.5$, but no oscillatory behavior was found.

At pH 1.30 (Fig. 4(a)) only period 1 oscillations are observed along the series, that ends with a potential jump to $E > 1.20 \text{ V}$. The characteristic pattern is shown in Fig. 4(d). Increasing the pH to 2.15 (Fig. 4(b)), besides the period 1, more two patterns can be observed (Fig. 4(b) and (f) in which high amplitude cycles are separated by small amplitude oscillations with one or two cycles. Finally, in pH 3.5 (Fig. 4(c)) oscillations begin with period 1 changing to the pattern described in Fig. 4(f). These more complex patterns were already observed during the oscillatory MER in H_2SO_4 under potential control [17] or other small organic molecules, such as formaldehyde [47], ethanol [13], ethylene glycol [15] and glycerol [16].

While the peak to peak amplitude of the period 1 oscillations in pH 1.30 is ca 250–300 mV, at pH 2.15 and 3.50 they decrease to ca. 100–150 mV, but with the same mean potential observed in pH 1.30. This effect is the opposite of that observed for ethylene glycol [6] and formic acid [12] in $\text{H}_2\text{SO}_4/\text{K}_2\text{SO}_4$ solutions, where the amplitude increases in the 0.25 to 2.00 pH range. Oscillatory MER carried out in $0.1 \text{ mol L}^{-1} \text{ HClO}_4$ containing distinct amounts of trifluoromethanesulfonate indicates that the mean potential in oscillations cycles is not affected by anion adsorption, but the amplitude of oscillations increases [48]. Herein, in the pH range from 1.30 to 3.50 the increase of H_2PO_4^- concentration is followed by the decrease of undissociated phosphoric acid (H_3PO_4) in the system [44]. Both H_3PO_4 and H_2PO_4^- adsorb on Pt surface [35] but hydrogen phosphates adsorption decreases with pH [34]. Thus, H_2PO_4^- adsorption instead of H_3PO_4 seems to be the responsible to the small amplitude at the beginning of temporal series in pH 2.15 and 3.50.

From regions of period 1 it is possible to estimate the oscillation frequencies (ω), i.e. the inverse of time between two maximum

potentials in a cycle. The time in which each series spent in period 1 was normalized to a zero to one scale (t_N), with zero being the onset of oscillatory behavior and one the time of oscillation extinction at pH 1.30 or the transition to more complex patterns in other pH values. The ω evolution in time (Fig. 5) reveals that oscillations become slow regardless the pH, but the decrease is more effective in pH 1.30. Mean values of 0.37 ± 0.08 , 0.50 ± 0.05 and $0.38 \pm 0.04 \text{ Hz}$ to pH 1.30, 2.15 and 3.50, respectively do not allow us to draw a pathway to the extinguishment of oscillatory behavior. Again, for the oscillatory electro-oxidation of ethylene glycol and formic acid, ω was found to increase with pH [6,12].

The insensitivity of ω with the pH could come from a compensation effect between the decrease of anions adsorption strength, which in principle should increase the reaction rate, and the CO_{ad} formation from methanol adsorption that is more facile in the absence of adsorbed anions. Examples of compensation effects in oscillatory electrochemical systems were already observed for ω changes with temperature during oscillatory methanol [28], formic acid [46,49] or ethylene glycol [15] electro-oxidation reactions.

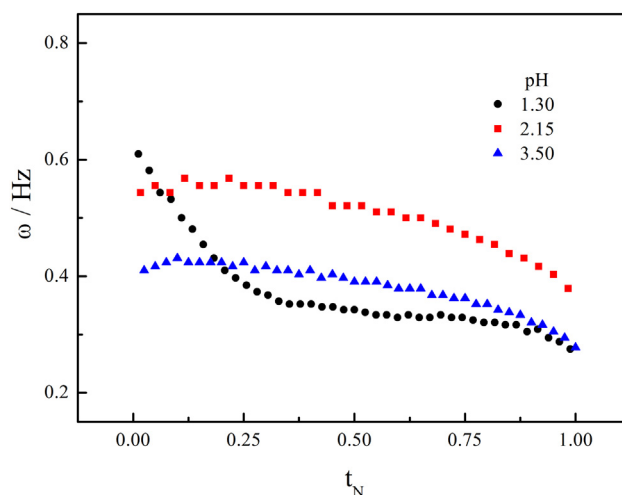


Fig. 5. Oscillation frequency (ω) along the P1 patterns depicted in the time series of Fig. 4.

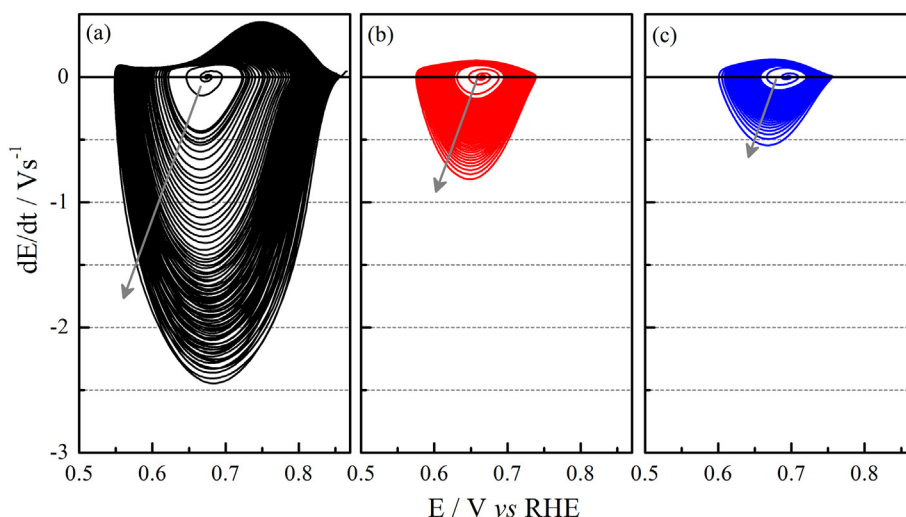


Fig. 6. dE/dt versus E profiles for period 1 patterns depicted in Fig. 4 for pH (a) 1.3, (b) 2.15 and (c) 3.50. The arrows indicate the time direction.

The rates of potential change in time (dE/dt) along one cycle of period 1 oscillations were calculated and plotted in terms of potential visited during oscillations (Fig. 6). This parameter can be associated with the poisoning/freeing rates of the surface since the current is kept constant and the potential should change in time to maintain the reaction rate [6,28,49,50]. Positive dE/dt rates represent the potential increase in an oscillation cycle to compensate the adsorption of poisoning species. On the other hand, negative values reflect the potential decrease after reaching their maximum value in the cycle, reflecting thus the removal of site-blocking adsorbates and the consequent freeing of the surface [28,50]. The asymmetric dE/dt versus E profiles indicates that poisoning and freeing of surface occur by distinct mechanisms, with the last one probably connected with autocatalytic processes of (hydro)oxides reduction by chemical interaction with methanol [51]. Fig. 6 also reveals high dE/dt values at pH 1.30 (with maximum positive value at 0.75 V) decreasing in pH 2.15 and 3.50. Showing the series in terms of dE/dt , the extinguishment of oscillatory behavior becomes a progressive process with the pH, suggesting that poisoning steps are suppressed/less active at high pH. The facilitated surface oxidation with increasing pH and therefore the enhancement of the direct oxidation pathway might be the reason for that behavior.

The increase of dE/dt with time (grey arrows) suggests higher poisoning/freeing rates as the time-series evolves. In situ ATR-SEIRAS experiments, in absence of adsorbing anions, revealed that CO_{ad} amounts decrease during this process [52], thus, irreversible oxide formation is the most probably process responsible for the changes in the oscillations along the series (also known as spontaneous drift) [23]. Supporting this fact, it is observed an increase in the mean potential for the oscillation cycles along the time series (Figs. S2 and S3). The influence of pH and anions on the platinum (hydro)oxides formation/reduction is well reported in literature under extreme pH conditions [53,54]. However, as mentioned above, MER mechanism in the presence of hydrogen phosphate anions is unclear. Experiments with in situ FTIR as well as distinct anions in oscillatory pH range are in course in order to understand the MER mechanism and the oscillations extinguishment.

4. Conclusions

The methanol electro-oxidation reaction catalyzed by Pt was studied in a wide pH range in buffered hydrogen phosphates solutions. The main observations are summarized below.

1 – Two oxidation peaks followed by a broad oxidation region are observed at $pH < 5$ along the positive going scans in cyclic voltammograms. The peaks reach the minimum values around $pH 4-6$,

excepting the peak 2 being suppressed at $pH > 5.0$. The current values exponentially increase from pH 5 to 11. The minimum activity region is also observed in experiments under current control and coincides with changes in the behavior of CO_{ad} and formic acid electro-oxidation reactions. The behavior of MER along the studied pH range seems to be the opposite of formic acid in similar electrolyte conditions.

2 – Potential and current oscillations are observed in $pH < 4$. These oscillations are of period 1 regardless the pH and more complex patterns in pH 2.15 and 3.50. The mean oscillation frequencies do not change significantly in the studied pH range, but the amplitude and potential window decrease with pH.

3 – dE/dt analysis revealed a monotonic decrease of poisoning/freeing rate as the pH changes from 1.3 to 3.50, which suggests the oscillatory behavior is extinguished by the suppression of poisoning rate processes.

Acknowledgments

The authors thank São Paulo Research Foundation (FAPESP) for the scholarship (#2014/08030-9) and financial support (#2013/07296-2, #2014/23916-3 and #2013/16930-7) National Council for Scientific and Technological Development (CNPq) is also acknowledged (#306151/2010-3 and #454897/2014-6) for financial support. GBM also thanks CNPq/PIBIC for the scholarship.

Appendix A. Supplementary data

Supplementary data to this article can be found online at <https://doi.org/10.1016/j.jelechem.2018.08.033>.

References

- [1] H. Varela, M.V.F. Delmonde, A.A. Zulke, The oscillatory electrooxidation of small organic molecules, in: T. Maiyalagan, V.S. Saji (Eds.), *Electrocatalysts for Low Temperature Fuel Cells: Fundamentals and Recent Trends*, Wiley-VHC, New York, 2017, pp. 145–163.
- [2] U. Krewer, T. Vidakovic-Koch, L. Rihko-Struckmann, Electrochemical oxidation of carbon-containing fuels and their dynamics in low-temperature fuel cells, *ChemPhysChem* 12 (14) (2011) 2518–2544.
- [3] K. Krischer, H. Varela, Oscillations and other dynamic instabilities, in: W. Vielstich, A. Lamm, H.A. Gasteiger (Eds.), *Handbook of Fuel Cells: Fundamentals, Technology and Applications*, John Wiley & Sons, Chichester, 2003, pp. 679–701.
- [4] P. Strasser, M. Eiswirth, M.T.M. Koper, Mechanistic classification of electrochemical oscillators - operational experimental strategy, *J. Electroanal. Chem.* 478 (1–2) (1999) 50–66.
- [5] E.G. Machado, H. Varela, Kinetic instabilities in electrocatalysis, in: K. Wandelt (Ed.), *Encyclopedia of Interfacial Chemistry*, Elsevier, 2018, pp. 701–718.
- [6] E. Sitta, R. Nagao, H. Varela, The electro-oxidation of ethylene glycol on platinum

- over a wide pH range: oscillations and temperature effects, *PLoS One* 8 (9) (2013).
- [7] S.C.S. Lai, S.E.F. Kleijn, F.T.Z. Ozturk, V.C.v.R. Vellinga, J. Koning, P. Rodriguez, M.T.M. Koper, Effects of electrolyte pH and composition on the ethanol electro-oxidation reaction, *Catal. Today* 154 (1–2) (2010) 92–104.
- [8] V.S. Bagotzky, Y.B. Vassilyew, Mechanism of electro-oxidation of methanol on platinum electrode, *Electrochim. Acta* 12 (9) (1967) 1323–1343.
- [9] J.S. Spendlow, A. Wieckowski, Electrocatalysis of oxygen reduction and small alcohol oxidation in alkaline media, *Phys. Chem. Chem. Phys.* 9 (21) (2007) 2654–2675.
- [10] Y. Kwon, S.C.S. Lai, P. Rodriguez, M.T.M. Koper, Electrocatalytic oxidation of alcohols on gold in alkaline media: base or gold catalysis? *J. Am. Chem. Soc.* 133 (18) (2011) 6914–6917.
- [11] V.H. Günther, L. Müller, R. Wetzel, Oszillatorisches Verhalten der Formiatoxidation unter potentiostatischen Bedingungen, *Z. Phys. Chem.* 263 (6) (1982) 1121–1130.
- [12] F.W. Hartl, H. Varela, The effect of solution pH and temperature on the oscillatory electro-oxidation of formic acid on platinum, *Chemistryselect* 2 (27) (2017) 8679–8685.
- [13] L.F. Sallum, E.R. Gonzalez, J.M. Feliu, Potential oscillations during electro-oxidation of ethanol on platinum in alkaline media: the role of surface sites, *Electrochem. Commun.* 72 (2016) 83–86.
- [14] M.V.F. Delmonde, M.A. Nascimento, R. Nagao, D.A. Cantane, F.H.B. Lima, H. Varela, Production of volatile species during the oscillatory electro-oxidation of small organic molecules, *J. Phys. Chem. C* 118 (31) (2014) 17699–17709.
- [15] E. Sitta, M.A. Nascimento, H. Varela, Complex kinetics, high frequency oscillations and temperature compensation in the electro-oxidation of ethylene glycol on platinum, *Phys. Chem. Chem. Phys.* 12 (46) (2010) 15195–15206.
- [16] C.P. Oliveira, N.V. Lussari, E. Sitta, H. Varela, Oscillatory electro-oxidation of glycerol on platinum, *Electrochim. Acta* 85 (2012) 674–679.
- [17] A.L. Martins, B.C. Batista, E. Sitta, H. Varela, Oscillatory instabilities during the electrocatalytic oxidation of methanol on platinum, *J. Braz. Chem. Soc.* 19 (4) (2008) 679–687.
- [18] J. Lee, C. Eickes, M. Eiswirth, G. Ertl, Electrochemical oscillations in the methanol oxidation on Pt, *Electrochim. Acta* 47 (13–14) (2002) 2297–2301.
- [19] E.A. Carbonio, R. Nagao, E.R. Gonzalez, H. Varela, Temperature effects on the oscillatory electro-oxidation of methanol on platinum, *Phys. Chem. Chem. Phys.* 11 (4) (2009) 665–670.
- [20] R. Nagao, D.A. Cantane, F.H.B. Lima, H. Varela, Influence of anion adsorption on the parallel reaction pathways in the oscillatory electro-oxidation of methanol, *J. Phys. Chem. C* 117 (29) (2013) 15098–15105.
- [21] R. Nagao, D.A. Cantane, F.H.B. Lima, H. Varela, The dual pathway in action: decoupling parallel routes for CO₂ production during the oscillatory electro-oxidation of methanol, *Phys. Chem. Chem. Phys.* 14 (23) (2012) 8294–8298.
- [22] R. Nagao, R.G. Freitas, C.D. Silva, H. Varela, E.C. Pereira, Oscillatory electro-oxidation of methanol on nanoarchitected Pt-pc/Rh/Pt metallic multilayer, *ACS Catal.* 5 (2) (2015) 1045–1052.
- [23] R. Nagao, E. Sitta, H. Varela, Stabilizing nonstationary electrochemical time series, *J. Phys. Chem. C* 114 (50) (2010) 22262–22268.
- [24] W. Huang, Z.I. Li, Y.D. Peng, S. Chen, J.F. Zheng, Z.J. Niu, Oscillatory electrocatalytic oxidation of methanol on an Ni(OH)₂ film electrode, *J. Solid State Electrochem.* 9 (5) (2005) 284–289.
- [25] M.T.M. Koper, S.C.S. Lai, E. Herrero, Mechanisms of the oxidation of carbon monoxide and small organic molecules at metal electrodes, in: M.T.M. Koper (Ed.), *Fuel Cell Catalysis: A Surface Science Approach*, John Wiley & Son, Hoboken, 2009, pp. 159–207.
- [26] T. Iwasita, Electrocatalysis of methanol oxidation, *Electrochim. Acta* 47 (22–23) (2002) 3663–3674.
- [27] J.L. Cohen, D.J. Volpe, H.D. Abruna, Electrochemical determination of activation energies for methanol oxidation on polycrystalline platinum in acidic and alkaline electrolytes, *Phys. Chem. Chem. Phys.* 9 (1) (2007) 49–77.
- [28] F.W. Hartl, A.A. Zulke, B.J. Fonte, H. Varela, Temperature dependence of the evolving oscillations along the electrocatalytic oxidation of methanol, *J. Electroanal. Chem.* 800 (2017) 99–105.
- [29] K. Kunimatsu, H. Hanawa, H. Uchida, M. Watanabe, Role of adsorbed species in methanol oxidation on Pt studied by ATR-FTIRAS combined with linear potential sweep voltammetry, *J. Electroanal. Chem.* 632 (1–2) (2009) 109–119.
- [30] E.A. Batista, G.R.P. Malpass, A.J. Motheo, T. Iwasita, New mechanistic aspects of methanol oxidation, *J. Electroanal. Chem.* 571 (2) (2004) 273–282.
- [31] Z.Y. Zhou, N. Tian, Y.J. Chen, S.P. Chen, S.G. Sun, In situ rapid-scan time-resolved microscope FTIR spectroelectrochemistry: study of the dynamic processes of methanol oxidation on a nanostructured Pt electrode, *J. Electroanal. Chem.* 573 (1) (2004) 111–119.
- [32] E. Morallon, A. Rodes, J.L. Vazquez, J.M. Perez, Voltammetric and in-situ FTIR spectroscopy study of the oxidation of methanol on Pt(hkl) in alkaline media, *J. Electroanal. Chem.* 391 (1–2) (1995) 149–157.
- [33] R. Gisbert, G. Garcia, M.T.M. Koper, Oxidation of carbon monoxide on poly-oriented and single-crystalline platinum electrodes over a wide range of pH, *Electrochim. Acta* 56 (5) (2011) 2443–2449.
- [34] R. Gisbert, G. Garcia, M.T.M. Koper, Adsorption of phosphate species on poly-oriented Pt and Pt(111) electrodes over a wide range of pH, *Electrochim. Acta* 55 (27) (2010) 7961–7968.
- [35] F.C. Nart, T. Iwasita, On the adsorption of H₂PO₄⁻ and H₃PO₄ on platinum - an in-situ FT-IR study, *Electrochim. Acta* 37 (3) (1992) 385–391.
- [36] M.J.S. Farias, E. Herrero, J.M. Feliu, Site selectivity for CO adsorption and stripping on stepped and kinked platinum surfaces in alkaline medium, *J. Phys. Chem. C* 117 (6) (2013) 2903–2913.
- [37] G. Garcia, M.T.M. Koper, Carbon monoxide oxidation on Pt single crystal electrodes: understanding the catalysis for low temperature fuel cells, *ChemPhysChem* 12 (11) (2011) 2064–2072.
- [38] N.M. Markovic, P.N. Ross, Surface science studies of model fuel cell electrocatalysts, *Surf. Sci. Rep.* 45 (4–6) (2002) 121–229.
- [39] J.V. Perales-Rondon, E. Herrero, J.M. Feliu, Effects of the anion adsorption and pH on the formic acid oxidation reaction on Pt(111) electrodes, *Electrochim. Acta* 140 (2014) 511–517.
- [40] J. Joo, T. Uchida, A. Cuesta, M.T.M. Koper, M. Osawa, Importance of acid-base equilibrium in electrocatalytic oxidation of formic acid on platinum, *J. Am. Chem. Soc.* 135 (27) (2013) 9991–9994.
- [41] J. Joo, T. Uchida, A. Cuesta, M.T.M. Koper, M. Osawa, The effect of pH on the electrocatalytic oxidation of formic acid/formate on platinum: a mechanistic study by surface-enhanced infrared spectroscopy coupled with cyclic voltammetry, *Electrochim. Acta* 129 (2014) 127–136.
- [42] Y. Kwon, K.J.P. Schouten, M.T.M. Koper, Mechanism of the catalytic oxidation of glycerol on polycrystalline gold and platinum electrodes, *ChemCatChem* 3 (7) (2011) 1176–1185.
- [43] J.V. Perales-Rondon, S. Brimaud, J. Solla-Gullon, E. Herrero, R.J. Behm, J.M. Feliu, Further insights into the formic acid oxidation mechanism on platinum: pH and anion adsorption effects, *Electrochim. Acta* 180 (2015) 479–485.
- [44] D.A. Skoog, D.M. West, S.R. Crouch, F.J. Holler, *Fundamentals of Analytical Chemistry*, Brooks/Cole, Cengage Learning, 2014.
- [45] A. Cuesta, At least three contiguous atoms are necessary for CO formation during methanol electrooxidation on platinum, *J. Am. Chem. Soc.* 128 (41) (2006) 13332–13333.
- [46] R. Nagao, I.R. Epstein, E.R. Gonzalez, H. Varela, Temperature (over) compensation in an oscillatory surface reaction, *J. Phys. Chem. A* 112 (20) (2008) 4617–4624.
- [47] H. Okamoto, N. Tanaka, M. Naito, Chaotic and periodic potential oscillations in formaldehyde oxidation, *J. Phys. Chem. A* 102 (38) (1998) 7343–7352.
- [48] G.C.A. Ferreira, B.C. Batista, H. Varela, Experimental assessment of the sensitiveness of an electrochemical oscillator towards chemical perturbations, *PLoS One* 7 (11) (2012) e50145.
- [49] A.A. Zulke, H. Varela, The effect of temperature on the coupled slow and fast dynamics of an electrochemical oscillator, *Sci. Rep.* 6 (2016) 24553.
- [50] N. Perini, E. Sitta, A.C.D. Angelo, H. Varela, Electrocatalytic activity under oscillatory regime: the electro-oxidation of formic acid on ordered Pt₃Sn intermetallic phase, *Catal. Commun.* 30 (2013) 23–26.
- [51] B.C. Batista, E. Sitta, M. Eiswirth, H. Varela, Autocatalysis in the open circuit interaction of alcohol molecules with oxidized Pt surfaces, *Phys. Chem. Chem. Phys.* 10 (44) (2008) 6686–6692.
- [52] E. Boscheto, B.C. Batista, R.B. Lima, H. Varela, A surface-enhanced infrared absorption spectroscopic (SEIRAS) study of the oscillatory electro-oxidation of methanol on platinum, *J. Electroanal. Chem.* 642 (1) (2010) 17–21.
- [53] H. Angerstein-Kozłowska, B.E. Conway, B. Barnett, J. Mozota, Role of ion adsorption in surface oxide formation and reduction at noble-metal - general features of the surface process, *J. Electroanal. Chem.* 100 (1–2) (1979) 417–446.
- [54] B.E. Conway, Electrochemical oxide film formation at noble-metals as a surface-chemical process, *Prog. Surf. Sci.* 49 (4) (1995) 331–452.